

ANL Updates for the RIA Baseline Design

Kenneth W. Shepard
ANL Physics Division

Abstract

In the two and a half years since a baseline design for the RIA facility was outlined in the proceedings of the Harrison committee, ongoing research for the driver linac has identified both risks and opportunities that call for changing several of the types of SC cavity employed. The risk is emittance growth from beam-steering caused by the RF magnetic field in both of the two-drift-tube QWR-based cavities of the baseline design. We have replaced these structures with a single drift-tube, steering-corrected QWR cavity and with a half-wave cavity. The updated designs, in addition to reducing steering, have substantially lower peak-surface-magnetic fields, which removes an impediment to increasing the operating field level for these cavities. An increase is warranted by the excellent experimental results obtained in development of spoke-loaded cavities at Argonne and at other laboratories, and can be achieved by upgrading both the cavity processing and assembly techniques, and also the cavity operating environment.. This change would update the technology of the first two sections of the driver linac to be consistent with the technology of the third, high energy section. In addition, recent test results on a prototype multi-cell, double-spoke cavity for RIA confirm a possibility to replace the 805 MHz, elliptical-call cavities in the high-energy section with two types of multi-cell triple-spoke-loaded, 345 MHz cavities. Operating the high-energy section at lower-frequency would offer a number of advantages, including 1) a substantial reduction in the number of cavities required, 2) reduced refrigeration load, 3) operation at 4.2K, eliminating the need for sub-atmospheric cryogenics, and 4) a substantially increased longitudinal acceptance, decreasing the chances for beam loss due to straggling in the final stripper foil. Status of two prototype triple-spoke cavities will be discussed.

INTRODUCTION

This paper outlines changes to the baseline design for the U. S. RIA facility made over the last 30 months by the RIA design team at Argonne National Laboratory[1]. All of the changes discussed concern the cavity types and configuration of the 1.4 GeV driver linac, and we discuss them in the order which they were made.

The first design change was introduced at the time of the 2nd RIA Driver Workshop which changed the cavity configuration in the medium energy section of the linac, between the two stripper foils [2].

The second design change is being formally introduced at this workshop, which changes the cavity configuration of the high-energy, output section of the linac.

Many of the technical issues raised in this paper are discussed in more detail in other presentations at this workshop [3 – 7]. We note in particular that beam dynamics simulations are given only brief mention below, but that the design changes discussed have been numerically modeled in detail using full 3D fields, including alignment and

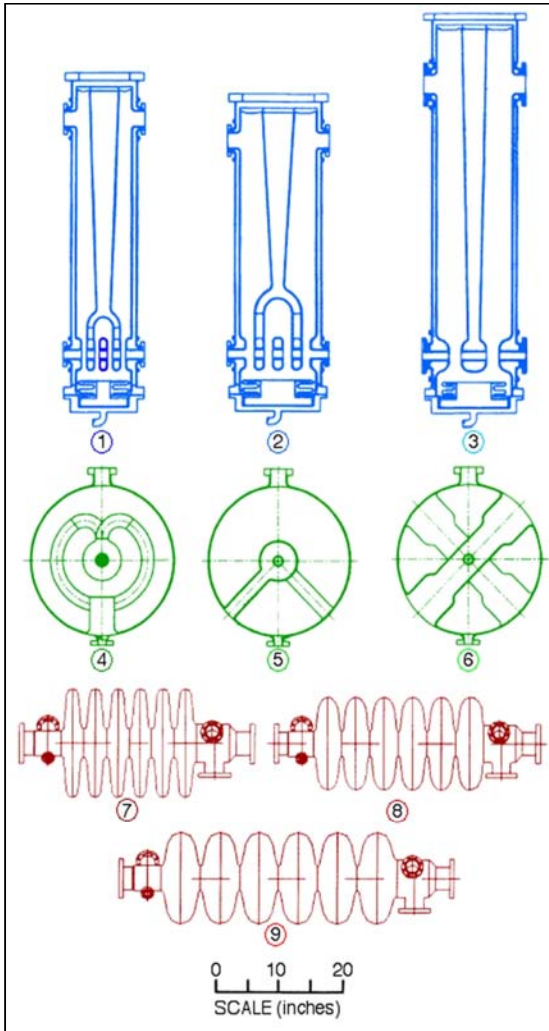


Figure 1 – Schematic outlines of the nine types of superconducting cavity required by the baseline design for the RIA driver linac.

this change we not only addressed the steering issue, but also created an opportunity for increasing the operating gradient by reducing the peak surface rf magnetic field in these structures.

Recent development tests of drift-tube cavities using high-pressure water rinse cleaning techniques indicate a substantial increase in surface electric field is possible (as is discussed below). In the originally proposed split-ring and lollipop cavities, various design constraints resulted in peak surface RF magnetic fields on the order of 750 gauss at the assumed accelerating gradients of 4 – 5 MV/m, which is at the limit of what has been achieved operationally in drift tube structures. In other words, the split-ring and lollipop are performance limited by the high peak *magnetic* field and cannot accommodate an increase in the operating peak surface *electric* field.

control errors, and space-charge effects where appropriate, as is discussed elsewhere in this workshop by Peter Ostroumov and his co-workers [8-12].

FIRST ANL UPDATE

Figure 1 shows in schematic outline the 9 types of superconducting cavity required by the RIA baseline design at the time of the Harrison cost review. The first six cavities are all drift-tube-loaded or TEM-class [14], are of relatively low frequency, assumed to operate at 4 K. The baseline specifications for accelerating gradients were limited to values that had been achieved in routine operation of recently constructed portions of existing SC ion linacs.

Detailed ray tracing through the cavities showed that beam deflection by rf magnetic fields can be problematic, particularly for the lighter ions[8]. Such steering effects are small in spoke-loaded and other types of half-wave cavities, but can be objectionably large in QWR cavities. Steering can be fairly well corrected in single drift-tube QWR cavities, but in two-drift-tube QWR structures, such as the lollipop and split ring (cavity types (4) and (5) in Figure 1) no adequate method of correction has been devised.

For this reason, we developed two alternative cavity designs, shown in Figure 2, to replace the above cavities. In making

The replacement QWR and HWR cavities can accommodate such an increase, so that as part of this driver design update we changed the specified operating gradient for the drift-tube cavities to a peak surface electric field of 20 MV/m. We have excepted from this change the four-gap interdigital cavities in order to postpone further development of these structures: this exception has little impact, since a total of only seven interdigital cavities are required.

Table I lists the cavity array parameters for the RIA driver linac. We note that the changes include:

- Changing two cavity types to eliminate the effects of beam steering and reduce peak surface fields.
- Upgrading cavity techniques to increase peak surface electric fields by 10 – 20%.
- A net reduction of 10% in the total number of SC cavities required for the driver.

SC Cavity Development at ANL

Construction of prototype cavities at Argonne is detailed in a paper at this workshop[3]. Niobium prototypes of the cavities shown in Figure 2 are nearly complete, and initial tests should be completed this calendar year.

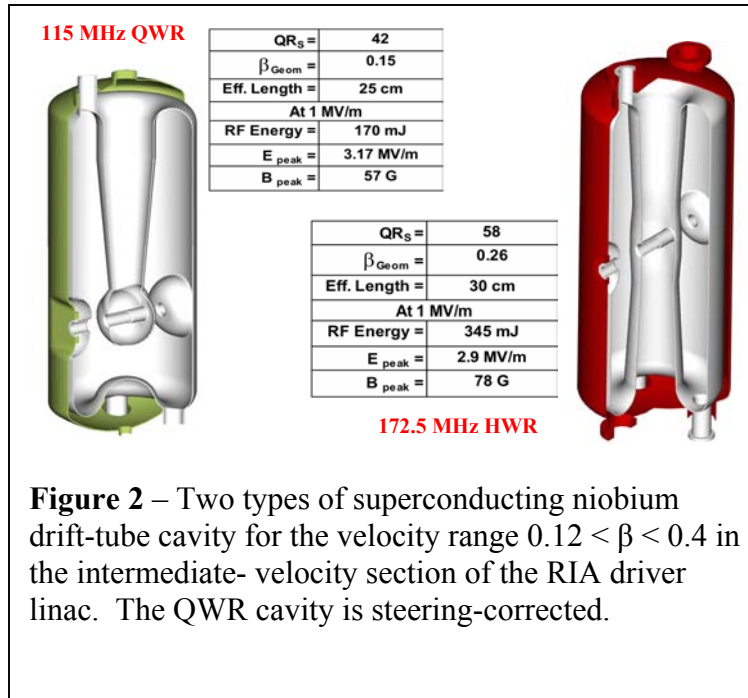


Figure 2 – Two types of superconducting niobium drift-tube cavity for the velocity range $0.12 < \beta < 0.4$ in the intermediate- velocity section of the RIA driver linac. The QWR cavity is steering-corrected.

Table 1 – Parameters of the cavity array for the 1st update RIA driver linac design

Type	Beta	Freq (MHz)	Length (cm)	at 1 MV/m		R/Q	G= QR _S	Maximum surface E field MV/m	Number of Cavities
				E _{PEAK}	B _{PEAK}				
Fork	0.02	58	20	3.8	99	1419	15	15.2	2
Fork	0.03	58	25	4.0	132	1177	17	16	5
QWR	0.06	58	20	3.0	58	714	21	20	28
QWR	0.15	115	25	3.2	57	509	42	20	48
HWR	0.26	173	30	2.9	78	241	58	20	80
2Spoke	0.39	345	38	3.3	70	444	87	20	56
6 Cell	0.47	805	53	3.4	69	160	137	27.5	54
6 Cell	0.61	805	68	2.7	57	279	179	27.5	88
6 Cell	0.81	805	91	2.2	47	483	260	27.5	32
Total # Cavities =									393

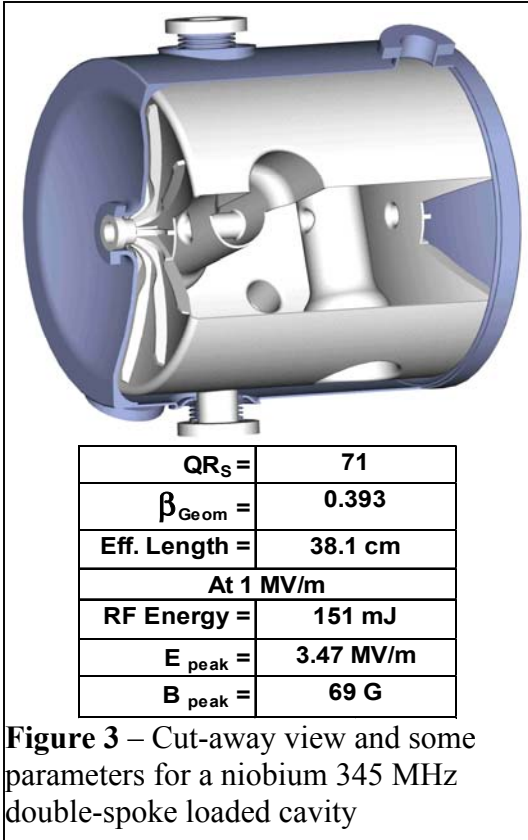


Figure 3 – Cut-away view and some parameters for a niobium 345 MHz double-spoke loaded cavity

Figure 3 shows the fifth cavity required by the driver, a 345 MHz double spoke loaded structure suitable for particle velocities $0.3 < \beta < 0.6$. The prototype for this cavity was recently completed, and some results of cold tests are shown in Figure 4. A more complete description of test results, including measurement of microphonic effects, is given in a paper at this workshop[4].

Several other laboratories have also recently obtained excellent results in 350 MHz (single) spoke-loaded cavities. Consistent operation at peak surface electric fields of 30 MV/m and above has been obtained by using high-pressure water rinsing and clean handling techniques.

SECOND ANL UPDATE

A 4K option for the RIA driver linac

The success achieved in increasing gradients in drift-tube loaded cavities has motivated us to develop designs for two types

of three-cell spoke-loaded cavity, or triple-spoke structure, suitable for the velocity range $0.4 < \beta < 0.75$, the high-energy section of the driver linac. Spoke-loaded cavities have about $\frac{1}{2}$ the diameter of elliptical-cell cavities at the same frequency and so, within a given radial constraint, can operate at $\frac{1}{2}$ the frequency. As is discussed below, this provides a number of advantages both in terms of performance and also of cost. One advantage is operation at 4.2K, so that we term this design option the 4k option for the driver linac[14].

Triple-spoke cavity design

Designs for two SC niobium, 345 MHz, three-spoke-loaded cavities have been developed. A sectioned view of one of the two cavity types is shown in Figure 5. The mechanical elements and overall design are similar to the recently prototyped 345 MHz two-spoke niobium cavity [4]. The niobium elements of the cavity are formed of 3.18 mm thick niobium sheet, and housed in an integral stainless-steel jacket, which contains the liquid helium coolant.

In the three lowest-frequency rf eigenmodes, the three spoke elements behave as

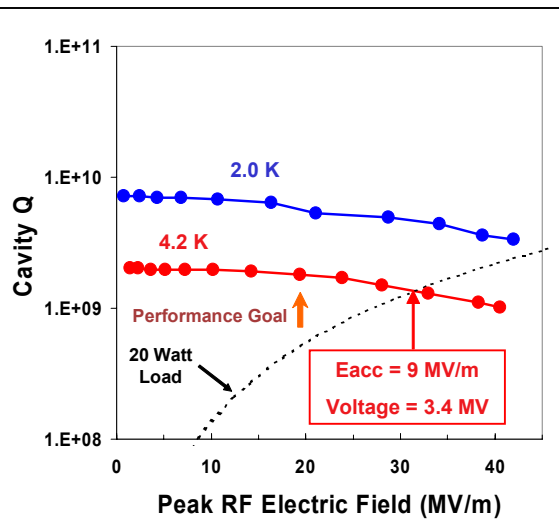


Figure 4 – Performance of the prototype niobium 345 MHz double-spoke cavity

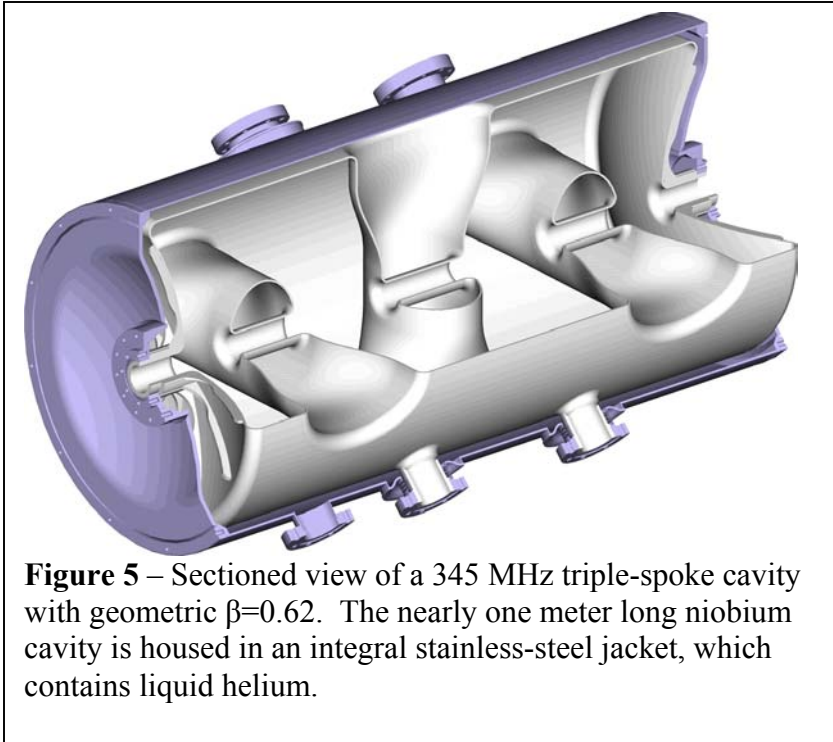


Figure 5 – Sectioned view of a 345 MHz triple-spoke cavity with geometric $\beta=0.62$. The nearly one meter long niobium cavity is housed in an integral stainless-steel jacket, which contains liquid helium.

coupled, TEM-like half-wave-resonant lines. Along each spoke, the rf electric field is radial and maximum in the middle of the spoke, decreasing to zero at either end. The rf magnetic field near each spoke is circumferential, with a maximum at either end and decreasing to zero at the middle. The lowest-frequency rf eigenmode is the accelerating mode, in which adjacent spokes are of opposing polarity.

Electromagnetic properties

The structures were modeled using Microwave Studio software. A primary design objective was to minimize and balance the peak values of surface electric and magnetic fields in order to maximize the accelerating gradient as constrained by present state-of-the-art for niobium SC cavities. As can be seen in Figure 5, the spoke elements are elliptical in cross-section. In the central portion of the spoke, the major axis is perpendicular to the beam axis, in order to minimize the peak value of the surface electric field. As the spoke approaches the cylindrical outer wall, elliptical section is expanded and the major axis rotates 90 degrees, parallel to the beam axis, in order to minimize the peak surface magnetic field.

A crossed-spoke geometry has been chosen in which the central spoke is oriented at a right angle to the spokes at each end of the cavity. It is possible to achieve approximately the same peak surface fields with all three spokes parallel, but the parallel-spoke geometry results in the lowest-lying rf eigenmodes being very closely spaced in frequency. The crossed-spoke geometry provides a large frequency spacing and maximizes the mechanical tolerances required to balance the electric fields in the three accelerating gaps. Also, the possibility of low-level multipacting coupling two rf modes is reduced with increased mode-splitting. For these reasons we have chosen the crossed-spoke geometry shown in Fig. 5.

Table 2 lists the principal electromagnetic parameters for the two 345 MHz triple-spoke-loaded cavities. Included for comparison are parameters for the two 805 MHz elliptical 6-cell cavities, designed for the same particle velocities, which are part of the ‘baseline’ design for the RIA driver linac.

Table 2: Electromagnetic parameters for the two triple-spoke cavities compared with two elliptical-cell 6-cell cavities of similar geometric $\beta = v/c$ developed for the SNS linac and for the RIA driver linac.

Cavity Type	Triple-Spoke	Elliptical Six-Cell	Triple-Spoke	Elliptical Six-Cell
Beta Geometric	0.50	0.47	0.62	0.61
Frequency (MHz)	345	805	345	805
Length (cm)	65.2	52.55	80.87	68.2
G (ohm)	85.7	136.7	93.0	179.0
R/Q = V^2/PQ (ohm)	494	160	520	279
at an accelerating gradient of 1 MV/m:				
RF Energy (mJ)	397	341	580	330
peak E-field (MV/m)	2.88	3.41	2.97	2.71
peak B-field (G)	86.5	69	88.6	57.2

Linac Configuration

We compare the ANL baseline driver linac design, which employs three types of 805 MHz elliptical-cell 6-cell cavities, and a design using the two types of triple-spoke-loaded cavity described above, i.e. 345 MHz, $\beta_{\text{GEOM}} = 0.5$ and 0.62 . In what follows we refer to the first option as the elliptical-cell linac (ECL) and the second option as the triple-spoke linac (TSL).

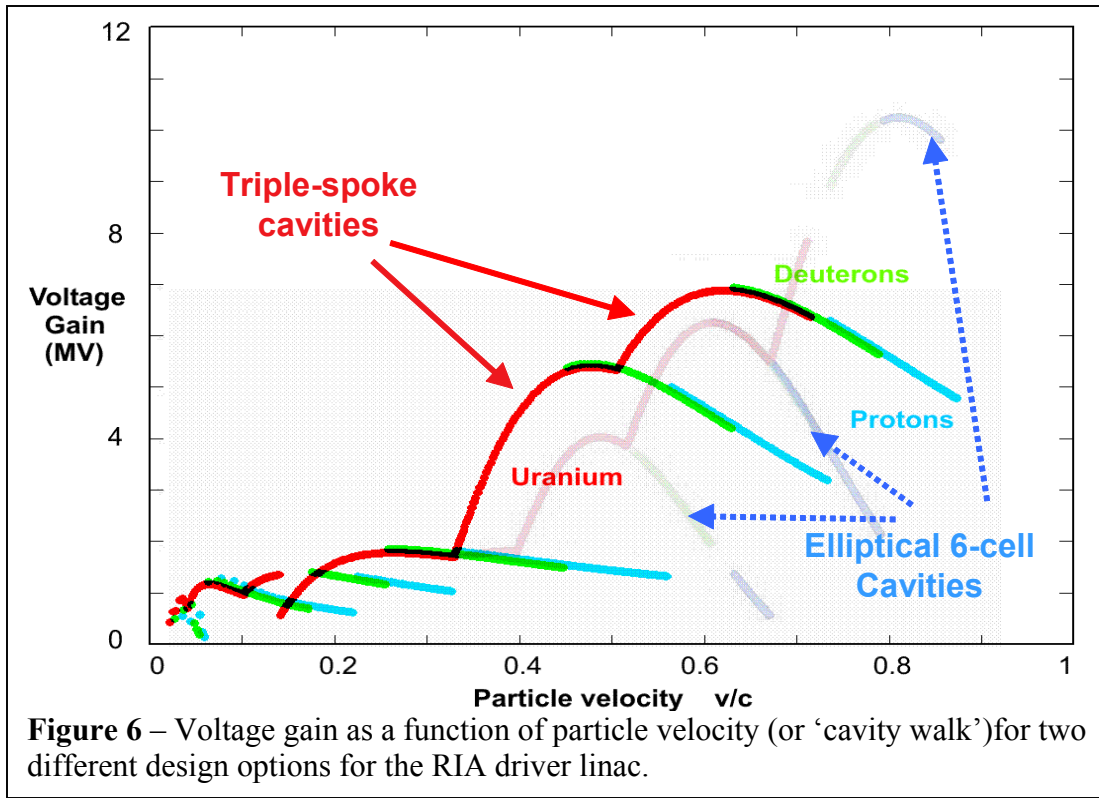


Table 3 - Parameter list for RIA driver cavities 4K design option using triple-spoke cavities.

Type	Beta	Freq (MHz)	Length (cm)	at 1 MV/m		R/Q	G = QR _s	Maximum surface E field (MV/m)	Number of Cavities
				E _{PEAK}	B _{PEAK}				
FORK	0.02	57.5	20	3.8	99	1419	15	15.2	2
FORK	0.03	57.5	25	4.0	132	1177	17	16	5
QWR	0.060	57.5	20	3.0	58	714	21	20	28
QWR	0.150	115.0	25	3.2	57	509	42	20	48
HWR	0.260	172.5	30	2.9	78	241	58	20	96
3SPOKE	0.500	345.0	65.2	2.9	65	494	86	27.50	69
3SPOKE	0.620	345.0	80.9	3.0	81	520	93	27.50	96
Total # of cavities =									344

Table 3 lists the cavity parameters for the latter (TSL) option. In Table 3 we assume operation of the triple-spoke cavities at the same maximum surface electric field of 27.5 MV/m assumed for the elliptical-cell cavities. The TSL option reduces the total cavity count from the ANL 1st update design by 49 cavities, and from the baseline design by 91 cavities.

Figure 6 compares the velocity acceptance, i.e. the voltage gain per cavity as a function of particle velocity, of the triple-spoke and elliptical-cell linac options. Note that, because of the lower frequency enabled by using a TEM structure, the triple-spoke geometry provides significantly broader velocity acceptance and higher voltage gain than the elliptical cell option.

The breadth of velocity acceptance varies inversely with the number of cells (each of length $\beta\lambda/2$) incorporated into accelerating structure. The more cells, the more voltage gain per cavity, but the narrower the velocity acceptance. In the present case, for a given particle velocity, the cell length is a factor of 2.33 longer for the 345 MHz three-cell spoke cavities, which can therefore provide at the same time both more voltage and broader velocity acceptance than an 805 MHz six-elliptical-cell cavity. As is discussed below, using these two triple-spoke cavities we can span the required velocity range not only with fewer cavities, but also with fewer types of cavity.

Table 4 compared output beam energies for the two design options, both of which are configured to produce 400 MeV/u uranium beams. The broad velocity acceptance of the TSL design provides a 71 MV higher energy proton beam than the ECL design.

Cavity RF heat load

The excellent shunt impedance of the spoke-loaded cavities, together with the relatively low operating frequency,

Table 4 – Comparison of beam output energies for several ion species for the two design options for the driver linac

Species	Energy (MeV/U)		Power (kW)
	E-cell	3-spoke	
H	912	983	400
He ³	716	733	400
D	590	591	400
O ¹⁸	537	533	400
Kr ⁸⁶	497	487	400
U ²³⁸	407	402	108

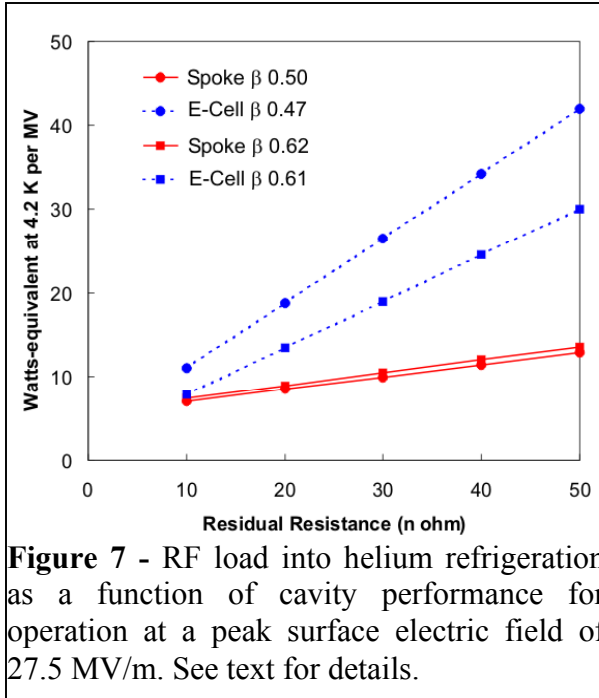


Figure 7 - RF load into helium refrigeration as a function of cavity performance for operation at a peak surface electric field of 27.5 MV/m. See text for details.

comparison, we show the refrigeration load for the 805 MHz elliptical six-cell cavities operating at 2K (dashed lines). The 2K system is assumed to achieve an efficiency such that a 0.25 watts into 2K is equivalent to 1 watts of heat load into 4.2K. The heat load in Figure 7 is estimated assuming operation of all cavities at a peak surface electric field of 27.5 MV/m, as discussed above.

In Figure 7, the heat load is shown as a function of cavity performance specified in terms of an empirically determined residual resistance characterizing the quality of the SC cavities. The residual resistance R_{EXC} is taken to be the resistance required to be added to the BCS SC surface resistance R_{BCS} [23] to account for the measured total rf loss ($R_{EXC} + R_{BCS}$) at a given temperature and field level. Design goals recently quoted for elliptical-cell cavities range over $25 < R_{EXC} < 50$ n Ω for long-term, on-line performance [x]. Actual production experience for sixteen 6-cell cavities for the SNS project has yielded a range $9 < R_{EXC} < 26$ n Ω in off-line, vertical cryostat tests. At this performance level, the use of spoke-loaded cavities would reduce the refrigeration load per MV of linac by a factor of two relative to the higher-frequency elliptical-cell alternative.

Note that for the spoke cavities, the reduced slope of heat load as a function of residual resistivity provides a large design margin in terms of overall linac heat-load as contingent on a range of SC cavity performance

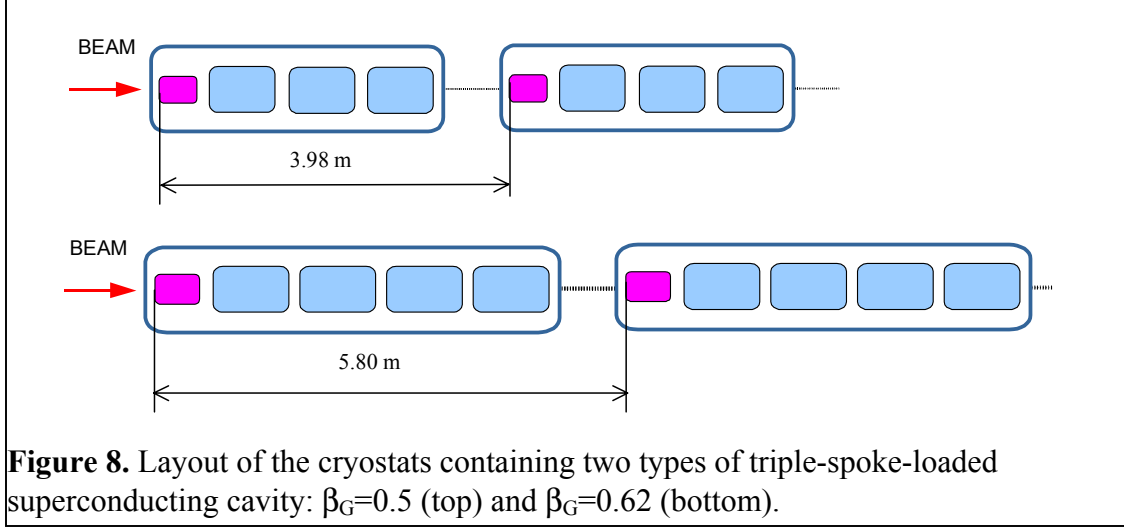
Linac lattice and beam loss

A potential issue with the triple-spoke cavity is that the 4 cm clear aperture is smaller than the 8 cm aperture required for adequate cell-to-cell coupling in the elliptical-cell structures. As we show below, the decrease in transverse acceptance is more than compensated by the increase in longitudinal acceptance provided by the lower frequency cavities [15].

enables us to design the linac not only to reduce the RF heat load but also to operate at 4.3K.

Operation at 4.2K is impractical for the elliptical-cell cavities which, because of the very much higher surface resistance at 805 MHz, must operate at 2K. The lower-frequency TEM spoke cavities can be operated at 4.2 K, which eliminates the need for sub-atmospheric operation, substantially simplifying the cryogenic system. The refrigerator, distribution system, and linac cryostats would all be appreciably simpler to build, maintain, and operate at a temperature of 4.2K as opposed to 2K.

Figure 7 shows the RF heat load in watts per MV of accelerating potential for the 345 MHz triple-spoke cavities operating at 4.2K (solid lines). For



A focusing system with room-temperature quadrupole doublets located outside of the cryostat is used in the ECL baseline design and could be used for the TSL. We have chosen, however, to use 50 cm long, 9 Tesla SC solenoids in the TSL design. The solenoids provide strong transverse focusing for all ion beams and can be incorporated into the resonator cryostats, economizing space along the beam-line.

A realistic accelerating-focusing lattice for the TSL high-energy section is based on two types of cryostat, as shown in Fig. 8. The first type is 3.4m in length and contains one SC solenoid and three $\beta_G=0.5$ triple-spoke cavities. The second type is 5.3m in length and contains one solenoid and four $\beta_G=0.62$ triple-spoke cavities. The space between the cryostats, approximately 0.5m, is adequate for beam diagnostics and beam steering magnets. We note that the latter could be integrated into the solenoids inside the cryostat. Table 5 summarizes and compares some of the principal parameters and features of the TSL and the ECL design options for the RIA driver linac high-energy section.

Beam dynamics were studied and compared for both design options by numerical modeling using the code TRACK, which integrates the particle motions through 3D electromagnetic fields. The 3D RF electromagnetic fields were obtained using electro-dynamics code CST Microwave Studio (Version 4.0).

In the simulations, the synchronous phase for the ECL is set at minus 30° , while in the TSL it can be reduced to minus 25° because of the large longitudinal acceptance of the lower-frequency cavity array.

In what follows we consider a

Table 5: Summary of the parameters for the two design options for the high-energy section of the RIA driver linac

<i>Parameter</i>	<i>Triple-spoke</i>	<i>Elliptical-cell</i>
Frequency (MHz)	345	805
No. of cavity types	7	9
Total no. of cavities	393	344
Temperature (K)	4.2	2
Aperture (mm)	40	80
Synchronous phase	-25	-30
<i>Normalized Acceptance</i>		
Trans. ($\pi \cdot \text{mm} \cdot \text{mrad}$)	35	70
Long. ($\pi \cdot \text{keV/u-nsec}$)	280	60

(worst-case) multiple-charge state uranium beam, with four charge states from the second stripper going through the high-energy section. The simulation results shown are for 10^4 particles per bunch and include 30 seeds of random errors both in alignment of all elements (300 micron), and also in the phase and amplitude of the electromagnetic fields in the SC cavities. The latter errors were set at a maximum of ± 1 degree and $\pm 1\%$ in the lowest frequency resonant cavities (58 MHz), and of ± 0.5 degree and $\pm 0.5\%$ in all higher frequency resonators.

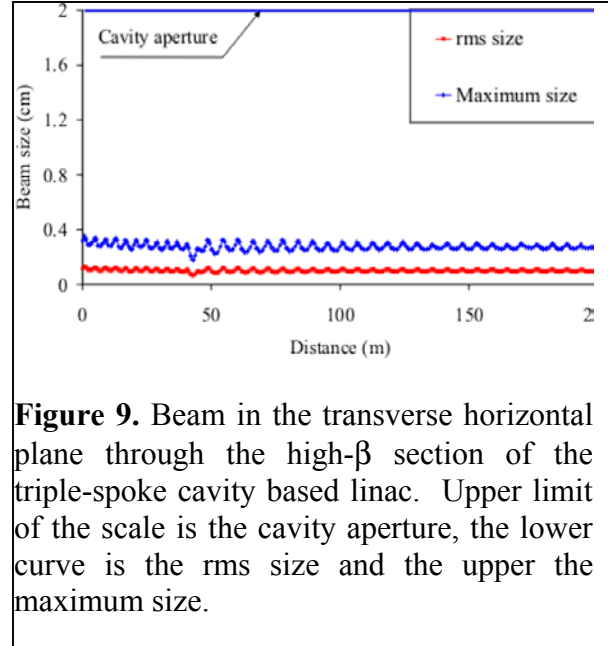


Figure 9. Beam in the transverse horizontal plane through the high- β section of the triple-spoke cavity based linac. Upper limit of the scale is the cavity aperture, the lower curve is the rms size and the upper the maximum size.

Figure 9 shows the transverse beam envelope through the high-energy section of the triple-spoke cavity based linac. Both rms and maximum transverse extent are shown, and indicate that the 4 cm aperture is ample for accommodating the worst-case multi-charge uranium beam.

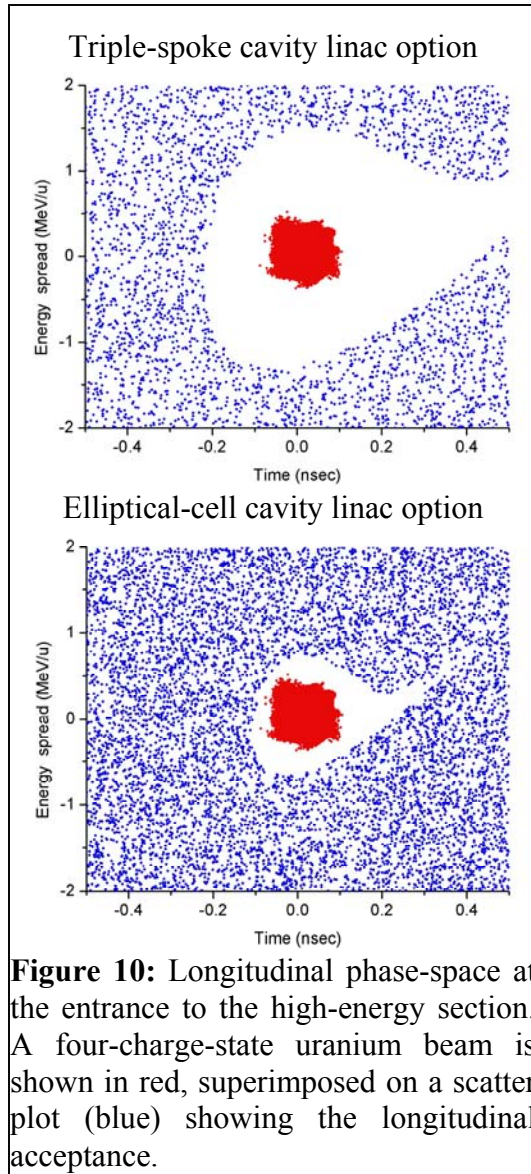


Figure 10: Longitudinal phase-space at the entrance to the high-energy section. A four-charge-state uranium beam is shown in red, superimposed on a scatter plot (blue) showing the longitudinal acceptance.

In Figure 10 the longitudinal acceptance for both the ECL and TSL designs, determined by Monte Carlo simulations, is outlined with blue dots. The red areas in Fig. 10 show, for both design options, the longitudinal phase-space of the four-charge-state uranium beam at the entrance of the high-energy section.

For the ECL design, the elliptical-cell iris diameter is set at 80 mm in order to provide adequate cell-cell coupling. Such a large aperture provides a very large transverse acceptance for this design option. The 40 mm beam aperture of the triple-spoke cavities provides, however, an ample safety factor in the transverse plane. Indeed, the aperture-to-rms-beam-size ratio, a critical factor for high-power linacs, remains in the range 16-20 throughout the TSL linac.

We note that the possibilities for beam loss are likely to be much more strongly impacted by the longitudinal rather than

transverse acceptance, since the situation is more marginal in longitudinal phase space. While the numerical studies reported to date indicate that both the baseline ECL and the TSL design options can provide good beam quality for multiple-charge-state beams, the reported studies have not included detailed simulation of the effects of scattering in the high energy stripping foil required for the heaviest ions.

The beam emittance shown in Figure 10 was obtained by, firstly, simulating the scattering in the foil numerically using the SRIM code. Secondly, the resultant estimates of transverse scattering and energy straggling were then used to generate the particle coordinates (just after the stripper), assuming Gaussian distribution in energy and scattered angles. The resultant standard deviations are 17.6 keV/u (energy) and 0.5 mrad (angle). Finally, we have assumed the stripping foil to fluctuate in thickness by $\pm 2.5\%$, uniformly distributed. Such fluctuations are caused by thermal deformations and by beam-induced sputtering of the foil itself. Thickness fluctuations contribute substantially to the emittance growth because the total energy loss is large (3.29 MeV/u).

As was discussed in the previous section, a good method to avoid beam loss from the low energy tail is to provide large longitudinal acceptance in the high-energy section. The TSL design option achieves this to a much greater extent than the baseline ECR design, which more than doubles the linac frequency right at the second stripper. The effect on longitudinal acceptance is an even larger factor, which, as shown in Fig. 10, for the TSL design is 4.7 times as large as the acceptance for the ECL option.

CONCLUSION

By using the results of recent SC cavity R&D, much of it performed explicitly for RIA, we can appreciably increase the accelerating gradients from the baseline design and realize substantial savings.

We find that for the cw, variable-velocity-profile, multiple-charge-state RIA driver linac, spoke-loaded cavities provide a number of advantages compared with the higher-frequency, elliptical-cell structures. In particular, the 2nd ANL RIA update design:

1. Reduces the required number of cavities substantially.
2. Reduces the number of cavity types in the high-energy section from 3 to 2
3. Increases the operating temperature from 2 to 4.2 K
4. Reduces the refrigeration load by approximately a factor of two.
5. Increases the longitudinal acceptance by a factor of 4.7, decreasing the possibilities for beam loss and activation.
6. Provides cavities with superior mechanical stability, minimizing the difficulty of tuning and phase control.

REFERENCES

1. J. A. Nolen, "The U.S. Rare Isotope Accelerator Project", *Proc. 2002 Linear Accelerator Conference*, Gyeongju, South Korea, August 2002
2. K. W. Shepard, "The RIA Driver Linac", *Proc. 2002 Linear Accelerator Conference*, Gyeongju, South Korea, August 2002
3. J. D. Fuerst, "Medium Beta Cavity and Cryomodule Prototyping for RIA", *in the proceedings of this workshop*.

4. M. Kelly, "Cavity Development for RIA", *in the proceedings of this workshop*.
5. G.P. Zinkann, RF Coupler and Tuner Design for the RIA Superconducting Cavities, *in the proceedings of this workshop*.
6. N.E. Vinogradov, "Progress with the Room Temperature Structures for the RIA Linacs, *in the proceedings of this workshop*
7. R.C. Pardo, "Driver and RIB Linac Diagnostics and Beam Tuning", *in the proceedings of this workshop*
8. P.N. Ostroumov, "Driver Linac Beam Dynamics", *in the proceedings of this workshop*
9. B. Mustapha, "Large Scale Computing for Beam Dynamics Simulations and Target Modeling", *in the proceedings of this workshop*.
10. E. S. Lessner, "Multiple-Charge-State-Beam Steering in the RIA Driver Linac, *in the proceedings of this workshop*.
11. P.N. Ostroumov, Front End of the RIA Driver Linac, *in the proceedings of this workshop*.
12. P.N. Ostroumov, "Development of a Low Charge-to-Mass Ratio Post-Accelerator for the RIA Project, *in the proceedings of this workshop*.
13. J. R. Delayen, "Medium Beta Superconducting Accelerating Structures", in *Proc. 4th Workshop on RF Superconductivity*, Tsukuba, Japan, August 1989, KEK Report 89-21, p. 249.
14. K. W. Shepard, P.N. Ostroumov, and J.R. Delayen, "High-Energy Ion Linacs Based on Superconducting Spoke Cavities", *to be published in Phys. Rev. Special Topics Accelerated Beams*.
15. P.N. Ostroumov, "Sources of Beam Halo Formation in Heavy-Ion Superconducting Linac", in *Proc. ICFA Advanced Beam Dynamics Workshop "Halo'03"*, May 19 - 23, 2003, Montauk, N.Y